

Impact of the LZ Experiment on the DM Phenomenology and Naturalness in the MSSM

Dongwei Li¹, Lei Meng², and Haijing Zhou^{2*}

¹*Fundamentals Department, Henan Police College, Zhengzhou 450046, China*

²*School of Physics, Henan Normal University, Henan Xinxiang 453007, China*

This paper uses approximate analytical formulas and numerical results with the bino-dominated dark matter (DM) as an example to analyze the impact of the LUX-ZEPLIN (LZ) experiment on the DM phenomenology and naturalness in the Minimal Supersymmetric Standard Model (MSSM). We conclude that the limitation of the latest LZ experiment worsens the naturalness of the MSSM, as the predictions of the Z -boson mass and DM relic density demonstrate, particularly in the regions where the correct DM relic density is obtained by the Z - or h -mediated resonant annihilations.

arXiv:2312.01594v4 [hep-ph] 25 Jun 2024

*Email: zhouhaijing0622@163.com

1 Introduction

Supersymmetric models of particle physics are renowned for providing an elegant solution to the daunting gauge hierarchy problem. The Minimal Supersymmetric Standard Model (MSSM), as the most economical supersymmetric expansion model, may provide a solid description of nature from the weak scale to energy scales associated with the grand unification [1], which also receives indirect experimental support from the measured strengths of weak-scale gauge couplings, measured value of the top quark mass, and discovery of an SM Higgs-like boson by ATLAS [2] and CMS [3] in 2012. However, this audacious extrapolation has suffered a string of serious setbacks because LHC and DM data have shown no signs of supersymmetric matter, which has led some physicists to question whether weak-scale SUSY really exists or at least to concede that it suffers diversiform unattractive fine tunings [4].

In the MSSM, the Z-boson mass is as follows [5]

$$\frac{m_Z^2}{2} = \frac{m_{H_d}^2 + \Sigma_d^d - (m_{H_u}^2 + \Sigma_u^u) \tan^2 \beta}{\tan^2 \beta - 1} - \mu^2, \quad (1.1)$$

where $m_{H_u}^2$ and $m_{H_d}^2$ are the soft SUSY-breaking (not physical) Higgs mass terms; μ is the superpotential higgsino mass term; $\tan \beta \equiv v_u/v_d$ is the ratio of Higgs field vevs; Σ_u^u and Σ_d^d include various independent radiative corrections [6]. Since the term $(m_{H_d}^2 + \Sigma_d^d)$ is suppressed by $\tan^2 \beta - 1$, for even moderate $\tan \beta$ values, Eq. (1.1) approximately reduces to

$$\frac{m_Z^2}{2} \simeq -(m_{H_u}^2 + \Sigma_u^u) - \mu^2. \quad (1.2)$$

To naturally achieve $m_Z \simeq 91.2$ GeV, $-m_{H_u}^2$, $-\mu^2$, and each contribution to $-\Sigma_u^u$ should be comparable in magnitude to $m_Z^2/2$. The extent of the comparability can be quantified using the electroweak fine tuning parameter [7]¹

$$\Delta_{EW} \equiv \max_i |C_i| / (M_Z^2/2), \quad (1.3)$$

where $C_{H_u} = -m_{H_u}^2$, $C_\mu = -\mu^2$, and $C_{\Sigma_u^u} = -\Sigma_u^u$. A lower value of Δ_{EW} implies less fine tuning, and $1/\Delta_{EW}$ is the percentage of fine tuning, *e.g.*, $\Delta_{EW} = 20$ corresponds to $\Delta_{EW}^{-1} = 5\%$ fine tuning among the terms that contribute to $m_Z^2/2$. Therefore, given the experimental lower bound, there is a general consensus that smaller values of $|\mu|$ are preferred in fine tuning issues. However, the current experiment limits impose a strong lower bound on $|\mu|$. For example, in 2017, the analysis of a global fit for the MSSM, which considered various experimental constraints² showed that $\mu > 350$ GeV was favored at a

¹Compared with the other two measures of EWFT (Δ_{BG} and Δ_{HS}) as shown in Ref. [7], Δ_{EW} is created from weak-scale SUSY parameters and consequently contains no information about any possible high-scale origin. Hence, Δ_{EW} is advantageous because it is model-independent, where any model that yields the same weak-scale mass spectrum will generate the same value of Δ_{EW} [8–10]. Meanwhile, $\Delta_{EW} < \Delta_{BG} \lesssim \Delta_{HS}$, *i.e.*, Δ_{EW} can be considered a lower bound on electroweak fine tuning [11]. Any model with a large value of Δ_{EW} is always fine tuned.

²These experimental constraints include those from the DM relic density, PandaX-II (2017) results for the SI cross section [12], PICO results for the SD cross section [13], and searches for supersymmetric particles at the 13-TeV LHC with 36 fb^{-1} data (especially the CMS analysis of the electroweakino production) [14].

95% confidence level (C.L.) [15]. This value of μ can induce a tuning of approximately 3% to predict the Z -boson mass. The studies in Ref. [16] showed that the Xenon-1T direct search limits [17] imposed a strong lower bound on $|\mu|$, particularly for $\mu > 0$ or when the masses of the heavy Higgs bosons of the MSSM were near their current limit from LHC searches. Ref. [18] demonstrated that μ should be larger than approximately 500 GeV for $M_1 < 0$ and 630 GeV for $M_1 > 100$ GeV considering the recent measurement of the muon anomalous magnetic moment at Fermilab [74], first results of the LUX-ZEPLIN (LZ) experiment in the direct search for DM [20], and rapid progress of the LHC search for supersymmetry [14, 21, 22]. In Ref. [23], systematic studies on DM in the hMSSM with a light gaugino/higgsino sector revealed that the stringent requirement of the conventional thermal paradigm as a mechanism to achieve the correct DM relic density had a significant impact on the viable parameter space, one of which is that the lower bounds of μ were elevated to approximately 500 GeV. These improved bounds imply a tuning of $\mathcal{O}(1\%)$ to predict the Z -boson mass.

In this paper, using the approximate analytical formulas and numerical results, we analyzed the DM phenomenology and associated unnaturalness in the MSSM in detail under the latest LZ experimental limits. The rest of this paper is organized as follows. Section 2 briefly introduces the neutralino sectors of the MSSM and demonstrates the DM scattering cross-sections with nucleons and annihilation for bino-like $\tilde{\chi}_1^0$ using the approximate analytical formulas. Section 3 briefly describes our scanning strategy and investigates the predictions for the surviving samples and properties of bino-dominated DM scenarios to understand the associated unnaturalness. Section 4 presents our conclusions.

2 Dark Matter Section in the MSSM

In the MSSM, the neutralino mass matrix in the basis of $\Psi^0 = (-i\tilde{B}^0, -i\tilde{W}^0, \tilde{H}_d^0, \tilde{H}_u^0)$ is [24]:

$$M_{\text{neut}} = \begin{pmatrix} M_1 & 0 & -c_\beta s_W m_Z & s_\beta s_W m_Z \\ 0 & M_2 & c_\beta c_W m_Z & -s_\beta c_W m_Z \\ -c_\beta s_W m_Z & c_\beta c_W m_Z & 0 & -\mu \\ s_\beta s_W m_Z & -s_\beta c_W m_Z & -\mu & 0 \end{pmatrix}, \quad (2.1)$$

where M_1 , M_2 , and μ are the soft SUSY-breaking mass parameters of the bino, wino, and higgsinos, respectively; m_Z is the Z -boson mass; θ_w is the Weinberg angle ($c_W \equiv \cos \theta_W$ and $s_W \equiv \sin \theta_W$); $\tan \beta \equiv s_\beta/c_\beta = v_u/v_d$ is the ratio of the vacuum expectation values for the two Higgs doublets ($c_\beta \equiv \cos \beta$ and $s_\beta \equiv \sin \beta$) and $v^2 = v_u^2 + v_d^2 = (246 \text{ GeV})^2$. Diagonalizing M_{neut} with a 4×4 unitary matrix N yields the masses of the physical states $\tilde{\chi}_i^0$ (ordered by mass) of four neutralinos:

$$N^* M_{\text{neut}} N^{-1} = \text{diag}\{m_{\tilde{\chi}_1^0}, m_{\tilde{\chi}_2^0}, m_{\tilde{\chi}_3^0}, m_{\tilde{\chi}_4^0}\}$$

with

$$\tilde{\chi}_i^0 = N_{i1}\tilde{B}^0 + N_{i2}\tilde{W}^0 + N_{i3}\tilde{H}_d^0 + N_{i4}\tilde{H}_u^0 \quad (i = 1, 2, 3, 4),$$

where $m_{\tilde{\chi}_i^0}$ is the root to the following eigenequation:

$$(x - M_1)(x - M_2)(x^2 - \mu^2) - m_{\tilde{Z}}^2(x - M_1 c_W^2 - M_2 s_W^2)(2\mu s_\beta c_\beta + x) = 0. \quad (2.2)$$

The eigenvector of $m_{\tilde{\chi}_i^0}$ is the column vector constituted by N_{ij} ($j = 1, 2, 3, 4$), which is given by

$$N_i = \frac{1}{\sqrt{C_i}} \begin{pmatrix} (\mu^2 - m_{\tilde{\chi}_i^0}^2)(M_2 - m_{\tilde{\chi}_i^0})s_W \\ -(\mu^2 - m_{\tilde{\chi}_i^0}^2)(M_1 - m_{\tilde{\chi}_i^0})c_W \\ (M_2 s_W^2 + M_1 c_W^2 - m_{\tilde{\chi}_i^0})(m_{\tilde{\chi}_i^0} c_\beta + \mu s_\beta)m_Z \\ -(M_2 s_W^2 + M_1 c_W^2 - m_{\tilde{\chi}_i^0})(m_{\tilde{\chi}_i^0} s_\beta + \mu c_\beta)m_Z \end{pmatrix}. \quad (2.3)$$

The specific form of the normalization factor C_i is:

$$C_i = (\mu^2 - m_{\tilde{\chi}_i^0}^2)^2 (M_2 - m_{\tilde{\chi}_i^0})^2 s_W^2 + (\mu^2 - m_{\tilde{\chi}_i^0}^2)^2 (M_1 - m_{\tilde{\chi}_i^0})^2 c_W^2 \\ + (M_2 s_W^2 + M_1 c_W^2 - m_{\tilde{\chi}_i^0})^2 (\mu^2 + m_{\tilde{\chi}_i^0}^2 + 4\mu m_{\tilde{\chi}_i^0} s_\beta c_\beta) m_Z^2. \quad (2.4)$$

Then, the diagonalizing matrix is $N = \{N_1, N_2, N_3, N_4\}$, where $i = 1, 2, 3, 4$ denotes the i -th neutralino.

This work focuses on the lightest neutralino, $\tilde{\chi}_1^0$, which acts as the DM candidate. N_{11}^2 , N_{12}^2 , and $N_{13}^2 + N_{14}^2$ are the bino, wino, and higgsino components in the physical state $\tilde{\chi}_1^0$, respectively, and satisfy $N_{11}^2 + N_{12}^2 + N_{13}^2 + N_{14}^2 = 1$. If $N_{11}^2 > 0.5$ ($N_{12}^2 > 0.5$ or $N_{13}^2 + N_{14}^2 > 0.5$), we call $\tilde{\chi}_1^0$ the bino- (wino- or higgsino-) dominant DM. The couplings of DM to the scalar Higgs states and Z-boson are included in the calculation of the DM-nucleon cross sections and DM annihilation, which correspond to the Lagrangian[25, 26]:

$$\mathcal{L}_{MSSM} \ni C_{\tilde{\chi}_1^0 \tilde{\chi}_1^0 h} h \tilde{\chi}_1^0 \tilde{\chi}_1^0 + C_{\tilde{\chi}_1^0 \tilde{\chi}_1^0 H} H \tilde{\chi}_1^0 \tilde{\chi}_1^0 + C_{\tilde{\chi}_1^0 \tilde{\chi}_1^0 Z} Z_\mu \tilde{\chi}_1^0 \gamma^\mu \gamma_5 \tilde{\chi}_1^0.$$

The coefficients are:

$$C_{\tilde{\chi}_1^0 \tilde{\chi}_1^0 h} \approx \frac{2m_Z^2 \mu}{v C_1} (\mu^2 - m_{\tilde{\chi}_1^0}^2) (M_2 s_W^2 + M_1 c_W^2 - m_{\tilde{\chi}_1^0})^2 \left(\frac{m_{\tilde{\chi}_1^0}}{\mu} + \sin 2\beta \right), \quad (2.5)$$

$$C_{\tilde{\chi}_1^0 \tilde{\chi}_1^0 H} \approx \frac{2m_Z^2 \mu}{v C_1} (\mu^2 - m_{\tilde{\chi}_1^0}^2) (M_2 s_W^2 + M_1 c_W^2 - m_{\tilde{\chi}_1^0})^2 \cos 2\beta, \quad (2.6)$$

$$C_{\tilde{\chi}_1^0 \tilde{\chi}_1^0 Z} \approx \frac{m_Z^3}{v C_1} (\mu^2 - m_{\tilde{\chi}_1^0}^2) (M_2 s_W^2 + M_1 c_W^2 - m_{\tilde{\chi}_1^0})^2 \cos 2\beta, \quad (2.7)$$

where h and H are two CP-even Higgs states predicted by the MSSM: the SM-like Higgs boson and non-SM doublet Higgs boson, respectively.

Serving as a weakly interacting massive particle (WIMP), $\tilde{\chi}_1^0$ may be detected by measuring their spin-independent (SI) and spin-dependent (SD) scattering cross-sections after an elastic scattering of $\tilde{\chi}_1^0$ on a nucleus occurs. At the tree level, the contribution to the SD (SI) scattering cross-section in the heavy squark limit is dominated by the t-channel Z-boson (CP-even Higgs bosons h_i) exchange diagram. Therefore, the scattering cross-sections have the following form [18, 27, 28]:

$$\sigma_{\tilde{\chi}_1^0-N}^{SD} \approx C_N \times \left(\frac{C_{\tilde{\chi}_1^0 \tilde{\chi}_1^0 Z}}{0.01} \right)^2, \quad (2.8)$$

$$\begin{aligned}
\sigma_{\tilde{\chi}_1^0-N}^{SI} &= \frac{m_N^2}{\pi v^2} \left(\frac{m_N m_{\tilde{\chi}_1^0}}{m_N + m_{\tilde{\chi}_1^0}} \right)^2 \left(\frac{1}{125 \text{GeV}} \right)^4 \times \\
&\quad \left\{ (F_u^N + F_d^N) C_{\tilde{\chi}_1^0 \tilde{\chi}_1^0 h} \left(\frac{125 \text{GeV}}{m_h} \right)^2 + \left(\frac{F_u^N}{\tan \beta} - F_d^N \tan \beta \right) C_{\tilde{\chi}_1^0 \tilde{\chi}_1^0 H} \left(\frac{125 \text{GeV}}{m_H} \right)^2 \right\}^2 \\
&\approx 6.4 \times 10^{-44} \text{cm}^2 \times \left(\frac{F_u^N + F_d^N}{0.28} \right)^2 \times \\
&\quad \left\{ \left(\frac{F_u^N}{F_u^N + F_d^N} \right) \times \left[\frac{C_{\tilde{\chi}_1^0 \tilde{\chi}_1^0 h}}{0.1} \left(\frac{125 \text{GeV}}{m_h} \right)^2 + \frac{1}{\tan \beta} \frac{C_{\tilde{\chi}_1^0 \tilde{\chi}_1^0 H}}{0.1} \left(\frac{125 \text{GeV}}{m_H} \right)^2 \right] \right. \\
&\quad \left. + \left(\frac{F_d^N}{F_u^N + F_d^N} \right) \times \left[\frac{C_{\tilde{\chi}_1^0 \tilde{\chi}_1^0 h}}{0.1} \left(\frac{125 \text{GeV}}{m_h} \right)^2 - \tan \beta \frac{C_{\tilde{\chi}_1^0 \tilde{\chi}_1^0 H}}{0.1} \left(\frac{125 \text{GeV}}{m_H} \right)^2 \right] \right\}^2, \quad (2.9)
\end{aligned}$$

where $N=p, n$ represents the proton and neutron, and $C_p \simeq 2.9 \times 10^{-41} \text{cm}^2$ ($C_n \simeq 2.3 \times 10^{-41} \text{cm}^2$) [29, 30]. The form factors at zero momentum transfer are $F_d^{(N)} = f_d^{(N)} + f_s^{(N)} + \frac{2}{27} f_G^{(N)}$ and $F_u^{(N)} = f_u^{(N)} + \frac{4}{27} f_G^{(N)}$, where $f_q^{(N)} = m_N^{-1} \langle N | m_q q \bar{q} | N \rangle$ ($q = u, d, s$) is the normalized light quark contribution to the nucleon mass, and $f_G^{(N)} = 1 - \sum_{q=u,d,s} f_q^{(N)}$ affects other heavy quark mass fractions in the nucleons [31, 32]. In this study, the default settings for $f_q^{(N)}$ were used in the micrOMEGAs package [33], and they predicted $F_u^p \simeq F_u^n \simeq 0.15$ and $F_d^p \simeq F_d^n \simeq 0.13$. Hence, the DM-proton scattering and DM-neutron scattering had approximately equal SI cross-sections (i.e., $\sigma_{\tilde{\chi}_1^0-p}^{SI} \simeq \sigma_{\tilde{\chi}_1^0-n}^{SI}$) [34].

In the pure bino limit ($m_{\tilde{\chi}_1^0} \approx M_1$ and $N_{11}^2 \approx 1$), the above formulas can be approximated as

$$C_1 = (\mu^2 - m_{\tilde{\chi}_1^0}^2)^2 (m_{\tilde{\chi}_1^0} - M_2)^2 s_W^2, \quad (2.10)$$

$$C_{\tilde{\chi}_1^0 \tilde{\chi}_1^0 h} \approx \frac{2m_Z^2 \mu s_W^2}{v(\mu^2 - m_{\tilde{\chi}_1^0}^2)} \left(\frac{m_{\tilde{\chi}_1^0}}{\mu} + \sin 2\beta \right), \quad (2.11)$$

$$C_{\tilde{\chi}_1^0 \tilde{\chi}_1^0 H} \approx \frac{2m_Z^2 \mu s_W^2}{v(\mu^2 - m_{\tilde{\chi}_1^0}^2)} \cos 2\beta, \quad (2.12)$$

$$C_{\tilde{\chi}_1^0 \tilde{\chi}_1^0 Z} \approx \frac{m_Z^3 s_W^2}{v(\mu^2 - m_{\tilde{\chi}_1^0}^2)} \cos 2\beta. \quad (2.13)$$

Meanwhile, taking $F_d^{(N)} \simeq F_u^{(N)} \simeq 0.14$ [35] and $\tan \beta \gg 1$, we can conclude that

$$\sigma_{\tilde{\chi}_1^0-n}^{SD} \approx 2.4 \times 10^{-40} \text{cm}^2 \times \frac{m_Z^2 v^2}{\mu^4} \times \left(\frac{1}{1 - m_{\tilde{\chi}_1^0}^2/\mu^2} \right)^2, \quad (2.14)$$

$$\begin{aligned}
\sigma_{\tilde{\chi}_1^0-N}^{SI} &\approx 2.1 \times 10^{-45} \text{cm}^2 \times \frac{v^2}{\mu^2} \times \left(\frac{1}{1 - m_{\tilde{\chi}_1^0}^2/\mu^2} \right)^2 \\
&\quad \times \left\{ \left(\frac{m_{\tilde{\chi}_1^0}}{\mu} + \sin 2\beta \right) \left(\frac{125 \text{GeV}}{m_h} \right)^2 + \frac{\tan \beta}{2} \left(\frac{125 \text{GeV}}{m_H} \right)^2 \right\}^2. \quad (2.15)
\end{aligned}$$

These two analytic formulas suggest that σ^{SD} and σ^{SI} are suppressed by μ^4 and μ^2 , respectively. Moreover, if $(\frac{m_{\tilde{\chi}_1^0}}{\mu} + \sin 2\beta)$ and $\tan \beta$ have opposite signs, the contributions to

σ^{SI} from the light Higgs(h) and heavy Higgs(H) exchange channels destructively interfere with each other. σ^{SI} will vanish for $(\frac{m_{\tilde{\chi}_1^0}}{\mu} + \sin 2\beta) \left(\frac{1}{m_h}\right)^2 + \frac{\tan\beta}{2} \left(\frac{1}{m_H}\right)^2 \rightarrow 0$, which is known as the “generalized blind spot” [28, 35]. For the convenience of subsequent descriptions, we defined $\mathcal{A}_h = (\frac{m_{\tilde{\chi}_1^0}}{\mu} + \sin 2\beta) \left(\frac{125\text{GeV}}{m_h}\right)^2$ and $\mathcal{A}_H = \frac{\tan\beta}{2} \left(\frac{125\text{GeV}}{m_H}\right)^2$ to represent the contributions from h and H to the SI cross-section, respectively.

For DM that was produced via the standard thermal freeze-out, the relic density at freeze-out temperature $T_F \equiv m_{\tilde{\chi}_1^0}/x_F$ (typically, $x_F \simeq 20$) was approximately [28]

$$\Omega_{\tilde{\chi}_1^0} h^2 \sim 0.12 \times \frac{2.5 \times 10^{-26} \text{cm}^3/\text{s}}{\langle\sigma v\rangle_{x_F}}, \quad (2.16)$$

where $\langle\sigma v\rangle_{x_F}$ corresponds to the effective (thermally averaged) annihilation cross-section. To match the observed DM relic density ($\Omega_{\text{DM}} h^2 \simeq 0.12$) [36], $\langle\sigma v\rangle_{x_F} \sim 2.5 \times 10^{-26} \text{cm}^3/\text{s}$ is required.

In the MSSM, for $m_{\tilde{\chi}_1^0} < 1$ TeV, only the bino-dominated $\tilde{\chi}_1^0$ can predict the correct DM relic density. For the higgsino- or wino-dominated $\tilde{\chi}_1^0$, the predicted relic density is much smaller than the observed DM relic density because they relatively strongly interacted with the Standard Model particles [37]. In our scenario, considering bino-like $\tilde{\chi}_1^0$ as an example, we will discuss the fine tunings introduced by the DM sector in the MSSM under the current DM experimental limits. For bino-like $\tilde{\chi}_1^0$, the contributions to $\langle\sigma v\rangle_{x_F}$ are from two channels

- The Z - or h -mediated resonant annihilation [38, 39]. The corresponding annihilation cross-sections are approximated to [40]

$$\langle\sigma v\rangle_{x_F}^{d\bar{d},Z} \sim (2.5 \times 10^{-26} \frac{\text{cm}^3}{\text{s}}) \times \left[\left(\frac{0.46 m_d}{1 \text{GeV}} \right) \times \frac{C_{\tilde{\chi}_1^0 \tilde{\chi}_1^0 Z}}{\left(1 - \frac{m_Z^2}{4m_{\tilde{\chi}_1^0}^2}\right)} \right]^2 \left(\frac{m_{\tilde{\chi}_1^0}}{46 \text{GeV}} \right)^{-4}, \quad (2.17)$$

$$\langle\sigma v\rangle_{x_F}^{d\bar{d},h} \sim (2.5 \times 10^{-26} \frac{\text{cm}^3}{\text{s}}) \times \left[\left(\frac{0.048 m_d}{1 \text{GeV}} \right) \times \frac{C_{\tilde{\chi}_1^0 \tilde{\chi}_1^0 h}}{\left(1 - \frac{m_h^2}{4m_{\tilde{\chi}_1^0}^2}\right)} \right]^2 \left(\frac{m_{\tilde{\chi}_1^0}}{62 \text{GeV}} \right)^{-2}. \quad (2.18)$$

Due to the hierarchy of Yukawa couplings, the contribution to the thermal cross-section from the $(\tilde{\chi}_1^0 \tilde{\chi}_1^0 \rightarrow q\bar{q})$ annihilations will be dominated by bottom quarks for the lighter $m_{\tilde{\chi}_1^0}$. Here, m_d is the down-type quark mass. As the expression shows, the measured relic density requires a high degeneracy between $m_{Z(h)}$ and $2m_{\tilde{\chi}_1^0}$. We define degeneracy parameters $\Delta_{Z(h)} = \left|1 - \frac{m_{Z(h)}^2}{4m_{\tilde{\chi}_1^0}^2}\right|$ to quantize the fine tuning between $m_{Z(h)}$ and $2m_{\tilde{\chi}_1^0}$, e.g., $\Delta_Z = 10^{-3}$ implies 0.1% fine tuning among m_Z and $2m_{\tilde{\chi}_1^0}$.

- Co-annihilation with sleptons, wino-dominated neutralinos, and/or charginos [18, 28, 38, 39, 42–46]. The corresponding reactions are $\tilde{\chi}_i \tilde{\chi}_j \rightarrow XX'$, where X and

X' donate SM particles. In this case, $\langle\sigma v\rangle_{x_F}$ in Eq. (2.16) should be replaced by $\langle\sigma_{eff}v\rangle_{x_F}$, and σ_{eff} is given by [41]

$$\sigma_{eff} = \sum_{i,j} \sigma_{ij} \frac{g_i g_j}{g_{eff}^2} (1 + \Delta_i)^{3/2} (1 + \Delta_j)^{3/2} \times \exp[-x(\Delta_i + \Delta_j)], \quad (2.19)$$

where

$$\sigma_{ij} = \sigma(\tilde{\chi}_i \tilde{\chi}_j \rightarrow X X'),$$

$$g_{eff} \equiv \sum_i g_i (1 + \Delta_i)^{3/2} \exp(-x \Delta_i),$$

$$\Delta_i \equiv (m_i - m_{\tilde{\chi}_1^0})/m_{\tilde{\chi}_1^0},$$

$x \equiv m_{\tilde{\chi}_1^0}/T$. g_i represents the internal degrees of freedom, and Δ_i parameterizes the mass splitting. In the co-annihilation case, the right relic abundance usually requires holding Δ_i at the 5 – 15% level [41], which also corresponds to one fine tuning.

3 Numerical Results and Theoretical Analysis

We used the MultiNest algorithm [47] with $n_{\text{live}} = 10000^3$ to comprehensively scan the following parameter space:

$$\begin{aligned} 1 \leq \tan \beta \leq 60, \quad 0.1 \text{ TeV} \leq \mu \leq 1 \text{ TeV}, \quad 0.5 \text{ TeV} \leq M_A \leq 10 \text{ TeV}, \\ -1.0 \text{ TeV} \leq M_1 \leq 1.0 \text{ TeV}, \quad 0.1 \text{ TeV} \leq M_2 \leq 1.5 \text{ TeV}, \\ -5 \text{ TeV} \leq A_t = A_b \leq 5 \text{ TeV}, \quad 0.1 \text{ TeV} \leq M_{\tilde{\mu}_L}, M_{\tilde{\mu}_R} \leq 1 \text{ TeV}, \end{aligned}$$

where $\tan \beta$ was defined at the electroweak scale, and the others were defined at the renormalization scale $Q = 1 \text{ TeV}$. To obtain the SM-like Higgs boson mass ($m_h \approx 125 \text{ GeV}$), the soft trilinear coefficients A_t and A_b were assumed to be equal and freely change to adjust the Higgs mass spectrum. The masses of the second-generation sleptons ($M_{\tilde{\mu}_L}, M_{\tilde{\mu}_R}$) were used as free parameters to explain the muon g-2 anomaly and predict the measured DM relic abundance by co-annihilation with sleptons. Other SUSY parameters of sleptons were fixed at 3 TeV to reduce the number of free parameters. The release of $\tilde{\tau}$ may change the e/μ signals of this study and relax the LHC restrictions [48, 49]. Other unimportant parameters were also fixed at 3 TeV, including the gluino mass M_3 and three generations of squarks except A_t and A_b .

During the scan, some experimental constraints were imposed by constructing the following corresponding likelihood function to guide the process as follows:

$$\mathcal{L} = \mathcal{L}_h \times \mathcal{L}_{h,\text{extra}} \times \mathcal{L}_B \times \mathcal{L}_{\Omega h^2} \times \mathcal{L}_{DD} \times \mathcal{L}_{Vac} \times \mathcal{L}_{a_\mu}, \quad (3.1)$$

where

³The n_{live} parameter in the algorithm controls the number of active points sampled in each iteration of the scan.

- \mathcal{L}_h and $\mathcal{L}_{h,\text{extra}}$ are the likelihood functions for the consistency of h 's properties with the LHC Higgs data at the 95% C.L. [53] and collider searches for extra Higgs bosons [57]. The two restrictions were implemented by the programs `HiggsSignal` 2.6.2 [50–53] and `HiggsBounds` 5.10.2 [54–57], respectively.
- \mathcal{L}_B is the likelihood function for the measured branching ratio of the $B \rightarrow X_s \gamma$ and $B_s \rightarrow \mu^+ \mu^-$. These ratios were calculated by the formulae in Refs. [58, 59] and should be consistent with their experimental measurements at the 2σ level [60].
- $\mathcal{L}_{\Omega h^2}$ is the likelihood function for the DM relic density with the central value of 0.120 from the Planck-2018 data [36]. We assumed theoretical uncertainties of 20% in the density calculation. \mathcal{L}_{DD} is the likelihood function for the 90% C.L. upper bounds of the PandaX-4T experiment on the SI DM-nucleon scattering [61] and XENON-1T experiment on the SD scattering [62]. These DM observables were calculated using the package `MicrOMEGAs` 5.0.4 [63–70].
- \mathcal{L}_{Vac} is the likelihood function for the vacuum stability of the scalar potential, which consists of the Higgs fields and the last two generations of the slepton fields. This condition was implemented by the code `Vevacious` [71, 72].
- \mathcal{L}_{a_μ} is the likelihood function of the muon $g - 2$ anomaly given by

$$\mathcal{L}_{a_\mu} \equiv \text{Exp} \left[-\frac{1}{2} \left(\frac{a_\mu^{\text{SUSY}} - \Delta a_\mu}{\delta a_\mu} \right)^2 \right] = \text{Exp} \left[-\frac{1}{2} \left(\frac{a_\mu^{\text{SUSY}} - 2.51 \times 10^{-9}}{5.9 \times 10^{-10}} \right)^2 \right],$$

where $\Delta a_\mu \equiv a_\mu^{\text{Exp}} - a_\mu^{\text{SM}}$ is the difference between experimental central value of a_μ and its SM prediction, and δa_μ is the total uncertainties in determining Δa_μ [73–75].

We defined $\mathcal{L} = 1$ if the restrictions were satisfied; otherwise, $\mathcal{L} = \text{Exp}[-100]$.

To probe into the impact of the LZ experiment on the DM phenomenology and naturalness of the complete parameter space in the MSSM, we did not consider the constraints from the LHC search for SUSY. Similar to the studies in Ref. [18], the restrictions from the LHC experiment require that the lower bounds of μ become approximately 400 GeV, and the upper bounds of M_1 become approximately 570 GeV, which severely compresses the surviving space of the MSSM. For example, compared with the restriction from the PandaX-4T experiment on the SI scattering cross-section, the lower bounds of μ improve by approximately 100 GeV. As a result, the regions with the Z - and h -mediated resonant annihilations are more unnatural at predicting the correct relic density so that they are commonly missed in the scans by the `MultiNest` algorithm.

The acquired samples were refined using the following criteria: the observed DM relic abundance within $\pm 10\%$ of the measured central value is $\Omega h^2 = 0.12$ (i.e., $0.108 \leq \Omega h^2 \leq 0.132$) [36], and $N_{11}^2 > 0.5$ to guarantee that the LSP is a bino-like neutralino. Then, we projected the refined samples on the corresponding planes of Fig. 1, Fig. 2 and Fig. 3.

In Fig. 1, we projected the surviving samples on the $m_{\tilde{\chi}_1^0} - \sigma_{\tilde{\chi}_1^0-p}^{SI}$ plane and $m_{\tilde{\chi}_1^0} - \sigma_{\tilde{\chi}_1^0-n}^{SD}$ plane, where the colors indicate the value of the higgsino mass μ . Fig. 1 shows that $\sigma_{\tilde{\chi}_1^0-n}^{SD}$ is

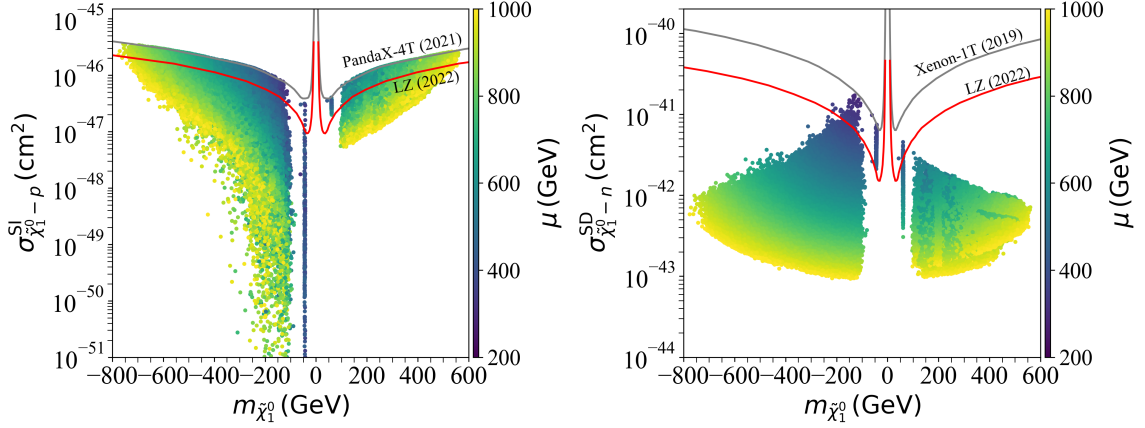


Figure 1. Projection of the refined samples onto $m_{\tilde{\chi}_1^0} - \sigma_{\tilde{\chi}_1^0-p}^{SI}$ (left panel) and $m_{\tilde{\chi}_1^0} - \sigma_{\tilde{\chi}_1^0-n}^{SD}$ (right panel). The colors indicate the value of the higgsino mass μ .

only related to μ and will be suppressed by a large μ , which is consistent with the analysis based on Eq. (2.14), i.e., $\sigma_{\tilde{\chi}_1^0-n}^{SD}$ is proportional to $\frac{m_Z^2 v^2}{\mu^4}$. The current LZ experiment constraint on $\sigma_{\tilde{\chi}_1^0-n}^{SD}$ requires that μ is greater than 370 GeV. However, the distribution of the $\sigma_{\tilde{\chi}_1^0-p}^{SI}$ values is relatively complex. Although large μ can suppress $\sigma_{\tilde{\chi}_1^0-p}^{SI}$, $\sigma_{\tilde{\chi}_1^0-p}^{SI}$ can also be small for small μ . Based on Eq. (2.15), $\sigma_{\tilde{\chi}_1^0-p}^{SI}$ should be related to a combination of M_1 , μ , $\tan\beta$, and m_H .

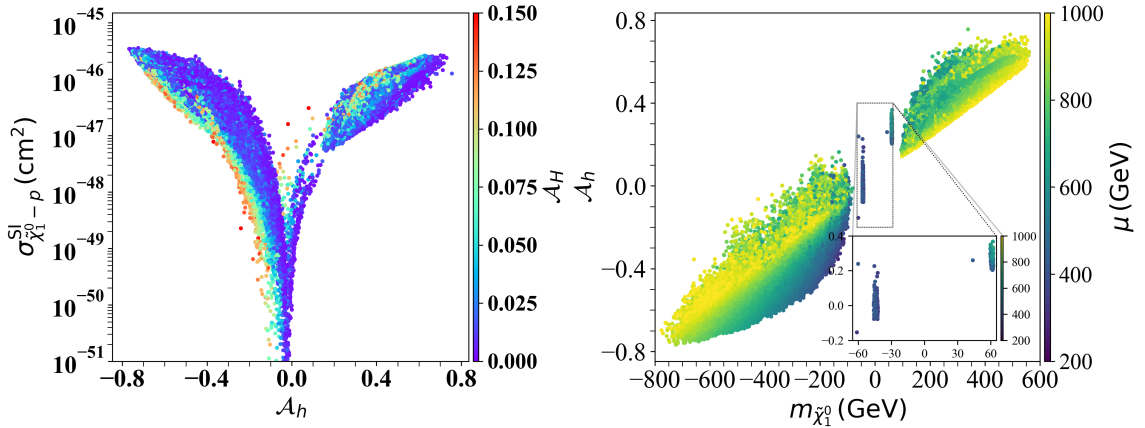


Figure 2. Projection of the refined samples onto the $\mathcal{A}_H - \sigma_{\tilde{\chi}_1^0-p}^{SI}$ plane, where the colors indicate the contributions from H to the SI cross-section \mathcal{A}_H , and onto the $m_{\tilde{\chi}_1^0} - \mathcal{A}_H$ plane, where the colors indicate the value of the higgsino mass μ .

To find the combination that will make $\sigma_{\tilde{\chi}_1^0-p}^{SI}$ satisfy the latest experimental limit, as presented in Fig. 2, we projected the surviving samples onto the $\mathcal{A}_H - \sigma_{\tilde{\chi}_1^0-p}^{SI}$ plane, where the colors indicate the contributions from H to the SI cross-section \mathcal{A}_H , and onto the $m_{\tilde{\chi}_1^0} - \mathcal{A}_H$ plane, where the colors indicate the value of the higgsino mass μ . The contribution of the heavy Higgs (H) to the SI cross-section for most samples was suppressed below 0.14 by

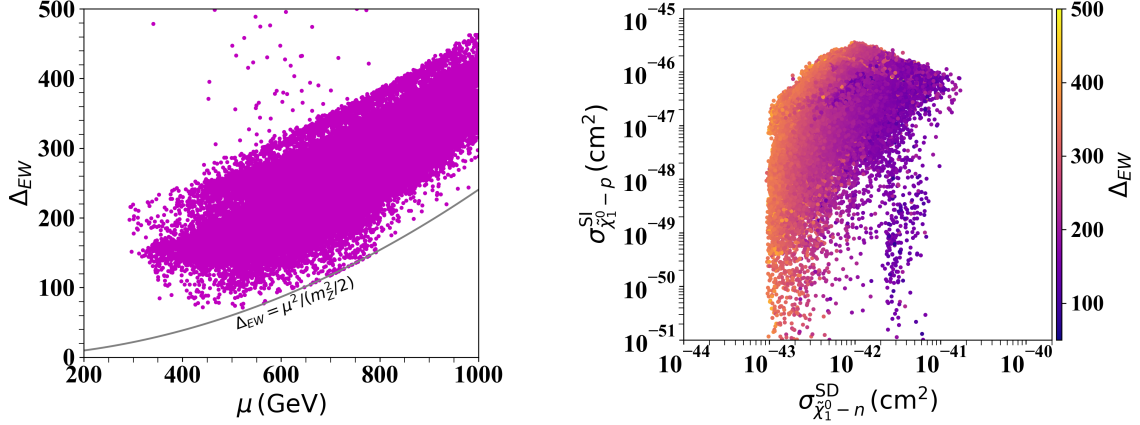


Figure 3. Projection of the refined samples onto the $\mu - \Delta_{EW}$ plane and $\sigma_{\tilde{\chi}_1^0-n}^{SD} - \sigma_{\tilde{\chi}_1^0-p}^{SI}$ plane with the colors indicating the values of Δ_{EW} .

m_H . Fig. 2 shows that compared with the contributions from H (\mathcal{A}_H) and v^2/μ^2 to the SI cross-section, the contribution of h (\mathcal{A}_h) played a dominant role.

In Fig. 3, we projected the samples onto the $\mu - \Delta_{EW}$ plane and $\sigma_{\tilde{\chi}_1^0-n}^{SD} - \sigma_{\tilde{\chi}_1^0-p}^{SI}$ plane with the colors indicating the values of EWFT (Δ_{EW}). Fig. 3 shows that the samples were fine-tuned with large $\Delta_{EW} > 70(\Delta_{EW}^{-1} = 1.4\%EWFT)$. According to the above discussion, the reason is that the latest LZ experiment requires $\mu > 370$ GeV. However, low Δ_{EW} solutions are only possible for low values of μ [7, 8]. As shown in the second figure of Fig. 3, Δ_{EW} of the samples allowed by the LZ experiment on the SI scattering cross-section may be relatively low due to the existence of the “generalized blind spot”. Because the values of $\mu^2/(m_Z^2/2)$ are the lower bounds of Δ_{EW} , we will use $\mu^2/(m_Z^2/2)$ to measure Δ_{EW} hereafter.

According to DM annihilation mechanisms, we divided the refined samples into four categories to discuss in detail.

1. Type-I samples: $m_{\tilde{\chi}_1^0} \approx -\frac{1}{2}m_Z$, $5 < \tan\beta < 58$, $337 \text{ GeV} < \mu < 462 \text{ GeV}$, $100 \text{ GeV} < M_2 < 1206 \text{ GeV}$. $\tilde{\chi}_1^0$ is mainly annihilated to $d\bar{d}$ by exchanging a resonant Z-boson in the s-channel to obtain its measured relic density. According to Eq. (2.17), the corresponding annihilation cross-section in this area is approximately

$$\langle\sigma v\rangle_{x_F}^{d\bar{d},Z} \simeq (2.5 \times 10^{-26} \frac{\text{cm}^3}{\text{s}}) \left[\frac{2.2 \times 10^{-3} \times C_{\tilde{\chi}_1^0\tilde{\chi}_1^0 Z}}{\Delta_Z} \right]^2 \left(\frac{m_{\tilde{\chi}_1^0}}{46 \text{ GeV}} \right)^{-4}. \quad (3.2)$$

From Fig. 1, $\sigma_{\tilde{\chi}_1^0-p}^{SI}$ can also satisfy the direct detection constraints with small μ values, but $\sigma_{\tilde{\chi}_1^0-n}^{SD}$ cannot. As discussed above, $\sigma_{\tilde{\chi}_1^0-p}^{SI}$ was proportional to $(\mathcal{A}_h + \mathcal{A}_H)$ and suppressed by μ^2 , so it even vanishes under the arranged limits of M_1 , μ , $\tan\beta$, and m_H . Fig. 2 shows that $|\mathcal{A}_h| < 0.1$, which corresponds to M_1/μ and $\tan\beta$ having opposite signs, e.g., suppresses the SI cross section. However, $\sigma_{\tilde{\chi}_1^0-n}^{SD}$ is only proportional to $\frac{m_Z^2 v^2}{\mu^4}$. According to Eq. (2.14), the LZ direct detection constraint on

the SD cross section requires $\mu > 500$ GeV for these samples, which corresponds to $\Delta_{EW}^{-1} = 1.7\%$. Further, according to Eqs. (2.13) and (3.2), $\mu = 500$ GeV corresponds to $C_{\tilde{\chi}_1^0 \tilde{\chi}_1^0 Z} = 3 \times 10^{-3}$, i.e., to predict the correct relic density, $\Delta_Z = 6.6 \times 10^{-6}$ which implies a tuning of $\mathcal{O}(0.0001\%)$. A larger μ corresponds to a more severe fine tuning, so μ cannot be very large in this case.

2. Type-II samples: $m_{\tilde{\chi}_1^0} \simeq \frac{1}{2}m_h$, $7 < \tan \beta < 33$, $406 \text{ GeV} < \mu < 776 \text{ GeV}$, $100 \text{ GeV} < M_2 < 994 \text{ GeV}$. $\tilde{\chi}_1^0$ is mainly annihilated to $b\bar{b}$ through the s-channel exchange of a resonant SM-like Higgs boson h to obtain its measured relic density. According to Eq. (2.18), the corresponding annihilation cross-section is approximated to

$$\langle \sigma v \rangle_{x_F}^{b\bar{b},h} \simeq (2.5 \times 10^{-26} \frac{\text{cm}^3}{\text{s}}) \left[\frac{0.2 \times C_{\tilde{\chi}_1^0 \tilde{\chi}_1^0 h}}{\Delta_h} \right]^2 \left(\frac{m_{\tilde{\chi}_1^0}}{62 \text{ GeV}} \right)^2. \quad (3.3)$$

Compared with the Type-I samples, the μ value increased in the case. For most samples, $\mu > 500$ GeV so that $\sigma_{\tilde{\chi}_1^0-n}^{SD}$ can satisfy the direct detection constraints, but $\sigma_{\tilde{\chi}_1^0-p}^{SI}$ cannot. From Fig. 2, the range of \mathcal{A}_h is (0.2,0.37), and the elevating effect of $(\mathcal{A}_h + \mathcal{A}_H)$ on $\sigma_{\tilde{\chi}_1^0-p}^{SI}$ has an advantage over the suppressing effect of μ^2 . At this time, M_1/μ and $\tan \beta$ have identical signs. For $\tan \beta = 10(30)$, according to Eq. (2.15), the direct detection constraints on the SI cross-section increased μ to above 1500 GeV (1200 GeV), which corresponded to $\Delta_{EW}^{-1} = 0.2\%$ ($\Delta_{EW}^{-1} = 0.3\%$). According to Eq. (2.11), for $\mu = 1500 \text{ GeV}$ (1200 GeV), $C_{\tilde{\chi}_1^0 \tilde{\chi}_1^0 h} = 3(4) \times 10^{-3}$, i.e., the right relic density requires $\Delta_h = 6(8) \times 10^{-4}$ which corresponds to a tuning of $\mathcal{O}(0.01\%)$.

3. Type-III and Type-IV samples: $m_{\tilde{\chi}_1^0} \in (-800, -100) \text{ GeV} \cup (100, 550) \text{ GeV}$, $5 < \tan \beta < 60$, $300 \text{ GeV} < \mu < 1000 \text{ GeV}$, $100 \text{ GeV} < M_2 < 1420 \text{ GeV}$, and $\tilde{\chi}_1^0$ is mainly co-annihilated with wino-dominated electroweakinos ($\tilde{\chi}_2^0$ or $\tilde{\chi}_1^\pm$) (Type-III samples) or sleptons ($\tilde{\mu}_L$ or $\tilde{\mu}_R$) (Type-IV samples) to achieve the measured density. Here, we used $\Delta_{M_2} = (M_2 - |m_{\tilde{\chi}_1^0}|)/|m_{\tilde{\chi}_1^0}|$, and $\Delta_{m_{\tilde{l}}} = (M_{\tilde{\mu}_L \text{ or } \tilde{\mu}_R} - |m_{\tilde{\chi}_1^0}|)/|m_{\tilde{\chi}_1^0}|$ to parameterize the mass splitting between $\tilde{\chi}_1^0$ and wino-dominated electroweakinos or sleptons. From Fig. 2, we can conclude that

- the cases with $-400 \text{ GeV} < m_{\tilde{\chi}_1^0} < -100 \text{ GeV}$ have the “generalized blind spot”, so $\sigma_{\tilde{\chi}_1^0-p}^{SI}$ can be small for small μ . However, the latest LZ experiment requires $\mu > 370 \text{ GeV}$. The right relic density requires $|\Delta_{M_2}| < 0.13$ or $|\Delta_{m_{\tilde{l}}}| < 0.18$.
- for the samples with $100 \text{ GeV} < m_{\tilde{\chi}_1^0} < 550 \text{ GeV}$, the contributions from h and H on $\sigma_{\tilde{\chi}_1^0-p}^{SI}$ reinforced each other so that $\sigma_{\tilde{\chi}_1^0-p}^{SI}$ was relatively large. The latest LZ experiment increased μ to above 582 GeV which corresponds to $\Delta_{EW}^{-1} = 1\%$. The right relic density requires $|\Delta_{M_2}| < 0.07$ or $|\Delta_{m_{\tilde{l}}}| < 0.07$.
- for the region with $-800 \text{ GeV} < m_{\tilde{\chi}_1^0} < -400 \text{ GeV}$, although M_1/μ and $\tan \beta$ have opposite signs, the values of $|\mathcal{A}_h|$ were too large so that $\sigma_{\tilde{\chi}_1^0-p}^{SI}$ remained

large for large μ . The latest LZ experiment also increased μ to above 600 GeV, and the right relic density is obtained when $|\Delta_{M_2}| < 0.07$ or $|\Delta_{m_{\tilde{t}}}| < 0.07$. Briefly, the characteristics of this area are similar to the cases with $100 \text{ GeV} < m_{\tilde{\chi}_1^0} < 550 \text{ GeV}$. Moreover, these regions of the parameter space will shrink or disappear with further improvement of sensitivity in future experiments.

Table 1. Values of μ and Δ_{EW} for four types of samples after and before considering the LZ experiment. \times and \surd indicate that the corresponding experimental limitations cannot and can be satisfied, respectively.

Sample type	Before		After				
	$\mu(\text{GeV})$	Δ_{EW}	SI		SD		
			$\mu(\text{GeV})$	Δ_{EW}	$\mu(\text{GeV})$	Δ_{EW}	
Type-I	(337,462)	(75,250)	(340,462)	(75,250)	\times	\times	
Type-II	(406,776)	(72,345)	\times	\times	(445,776)	(78,345)	
Type-III or IV	$M_1 < -400\text{GeV}$	(574,1000)	(117,452)	(607,1000)	(123,452)	\surd	\surd
	$-400\text{GeV} \lesssim M_1 \lesssim -100\text{GeV}$	(300,1000)	(71,500)	(300,1000)	(80,500)	(370,1000)	(71,500)
	$M_1 \gtrsim 100\text{GeV}$	(487,1000)	(122,463)	(582,1000)	(174,463)	\surd	\surd

Table 1 summarizes the above discussion of different samples. Δ_{EW} is the values presented in Fig.3. When the LZ experiment was considered, the lower bounds of the higgsino mass μ and Δ_{EW} were elevated, and μ should exceed 600 GeV, 370 GeV, 340 GeV, 440 GeV and 580 GeV for the cases of $M_1 < -400 \text{ GeV}$, $-400 \text{ GeV} \lesssim M_1 \lesssim -100 \text{ GeV}$, $M_1 \simeq -m_Z/2$, $M_1 \simeq m_h/2$, and $M_1 \gtrsim 100 \text{ GeV}$, respectively. In particular, μ was more tightly limited for the case of $M_1 > 0$ than for $M_1 < 0$, when $|M_1|$ was fixed. The reason is that, under the approximation $m_{\tilde{\chi}_1^0} \simeq M_1$, a negative M_1 can lead to the cancelation between different contributions to the SI DM-nucleon scattering cross-section in Eq. (2.15). These improved bounds of μ imply a tuning of $\mathcal{O}(1\%)$ to predict the Z -boson mass and simultaneously worsen the naturalness of the Z - or h -mediated resonant annihilations to achieve the measured DM relic density. When considering the restrictions from the LHC experiment, the lower bounds of μ improved by approximately 100 GeV, and the upper bound of M_1 was approximately 570 GeV [18], so the surviving region greatly decreased that will be exacerbated when future DM DD experiments fail to detect the signs of DM, which implies larger unnaturality of the MSSM.

4 Conclusion

In this study, the LZ experiment recently released its first results in the direct search for DM, where the sensitivities to the SI and SD cross-sections of DM-nucleon scattering reached approximately $6.0 \times 10^{-48} \text{ cm}^2$ and $1.0 \times 10^{-42} \text{ cm}^2$, respectively, for the DM mass of approximately 30 GeV [20]. These unprecedented precision values strongly limit the DM coupling to SM particles that are determined by the SUSY parameters. Considering this strong experimental limitation, the DM phenomenology and unnaturality related to DM physics in the MSSM were discussed in detail using approximate analytical formulas. It was found that under the limit of the latest dark matter experiment, the unnaturality

associated with DM in the MSSM is embodied in the large higgsino mass μ elevated by the latest LZ experiment requirement. For example, after considering the LZ experiment, the lower bounds of the higgsino mass μ and Δ_{EW} were elevated, and μ had to be larger than 600 GeV, 370 GeV, 340 GeV, 440 GeV and 580 GeV for the cases of $M_1 < -400$ GeV, -400 GeV $\lesssim M_1 \lesssim -100$ GeV, $M_1 \simeq -m_Z/2$, $M_1 \simeq m_h/2$, and $M_1 \gtrsim 100$ GeV, respectively. In particular, μ was more tightly limited for the case of $M_1 > 0$ than for $M_1 < 0$, when $|M_1|$ was fixed. These improved bounds of μ implied a tuning of $\mathcal{O}(1\%)$ to predict the Z -boson mass and simultaneously worsen the naturalness of the Z - and h -mediated resonant annihilations to achieve the correct DM relic density. If the LHC experiment is included, the surviving region greatly decreases which could be exacerbated if future DM DD experiments fail to detect the signs of DM, thus implying larger unnaturalness of the MSSM.

Acknowledgments

We sincerely thank Prof. Junjie Cao for numerous helpful discussions and his great effort to improve the manuscript. We thank LetPub for its linguistic assistance during the preparation of this manuscript. This work is supported by the Research and Practice Program on Research Teaching Reform in Undergraduate Colleges and Universities in Henan Province under Grant No.2022SYJXLX100, as well as the Research and Practice Program on Higher Education Teaching Reform in Henan Province under Grant No. 2024SJGLX0529.

References

- [1] S. P. Martin, In *Perspectives on supersymmetry II*, edited by G. L. Kane: 1-153 [hep-ph/9709356].
- [2] G. Aad *et al.* [ATLAS Collaboration], *Phys. Lett.* **B 716** (2012) 1.
- [3] S. Chatrchyan *et al.* [CMS Collaboration], *Phys. Lett.* **B 716** (2012) 30.
- [4] See *e.g.* M. Shifman, *Mod. Phys. Lett. A* **27** (2012) 1230043.
- [5] H. Baer and X. Tata, *Weak Scale Supersymmetry: From Superfields to Scattering Events*, (Cambridge University Press, 2006).
- [6] H. Baer, V. Barger, P. Huang, A. Mustafayev and X. Tata, *Phys. Rev. Lett.* **109** (2012) 161802; H. Baer, V. Barger, P. Huang, D. Mickelson, A. Mustafayev and X. Tata, arXiv:1212.2655 [hep-ph].
- [7] H. Baer, V. Barger and M. Padeffke-Kirkland, *Phys. Rev. D* **88** (2013), 055026 doi:10.1103/PhysRevD.88.055026 [arXiv:1304.6732 [hep-ph]].
- [8] H. Baer, V. Barger, P. Huang, D. Mickelson, A. Mustafayev and X. Tata, *Phys. Rev. D* **87** (2013) no.11, 115028 doi:10.1103/PhysRevD.87.115028 [arXiv:1212.2655 [hep-ph]].
- [9] H. Baer, V. Barger and D. Mickelson, *Phys. Rev. D* **88** (2013) no.9, 095013.
- [10] H. Baer, V. Barger, D. Mickelson and M. Padeffke-Kirkland, *Phys. Rev. D* **89** (2014) no.11, 115019.

- [11] H. Baer, V. Barger, P. Huang, D. Mickelson, A. Mustafayev and X. Tata, arXiv:1306.2926 [hep-ph].
- [12] X. Cui *et al.* [PandaX-II], Phys. Rev. Lett. **119** (2017) no.18, 181302 doi:10.1103/PhysRevLett.119.181302 [arXiv:1708.06917 [astro-ph.CO]].
- [13] C. Amole *et al.* [PICO], Phys. Rev. Lett. **118** (2017) no.25, 251301 doi:10.1103/PhysRevLett.118.251301 [arXiv:1702.07666 [astro-ph.CO]].
- [14] A. M. Sirunyan *et al.* [CMS], JHEP **03** (2018), 160 doi:10.1007/JHEP03(2018)160 [arXiv:1801.03957 [hep-ex]].
- [15] E. Bagnaschi, K. Sakurai, M. Borsato, O. Buchmueller, M. Citron, J. C. Costa, A. De Roeck, M. J. Dolan, J. R. Ellis and H. Flächer, *et al.* Eur. Phys. J. C **78** (2018) no.3, 256
- [16] M. Drees and G. Ghaffari, Phys. Rev. D **104** (2021) no.7, 075031 doi:10.1103/PhysRevD.104.075031 [arXiv:2103.15617 [hep-ph]].
- [17] E. Aprile *et al.* [XENON], Phys. Rev. Lett. **121** (2018) 111302, doi:10.1103/PhysRevLett.121.111302 [arXiv:1805.12562 [astro-ph.CO]].
- [18] Y. He, L. Meng, Y. Yue and D. Zhang, [arXiv:2303.02360 [hep-ph]].
- [19] MUON G-2 collaboration, B. Abi *et al.*, Phys. Rev. Lett. **126** (2021) 141801.
- [20] LZ collaboration, J. Aalbers *et al.*, 2207.03764.
- [21] ATLAS collaboration, G. Aad *et al.*, Eur. Phys. J. C **81** (2021) 1118.
- [22] CMS collaboration, A. M. Sirunyan *et al.*, JHEP **03** (2018) 166
- [23] G. Arcadi, A. Djouadi, H. J. He, J. L. Kneur and R. Q. Xiao, JHEP **05**, 095 (2023) doi:10.1007/JHEP05(2023)095 [arXiv:2206.11881 [hep-ph]].
- [24] A. Pierce, N. R. Shah and K. Freese, [arXiv:1309.7351 [hep-ph]].
- [25] H. E. Haber and G. L. Kane. Phys. Rept. **117** (1985) 75.
- [26] J.F. Gunion and H.E. Haber. Nucl. Phys. B **272** (1986) 1[Nuclear Physics B 402.1-2(1993):569].
- [27] S. Baum, M. Carena, N. R. Shah, and C. E. M. Wagner, JHEP **01** (2022) 025.
- [28] S. Baum, M. Carena, T. Ou, D. Rocha, N. R. Shah and C. E. M. Wagner, JHEP **11** (2023), 037 doi:10.1007/JHEP11(2023)037 [arXiv:2303.01523 [hep-ph]].
- [29] M. Badziak, M. Olechowski and P. Szczerbiak, JHEP **1603**, 179 (2016) doi:10.1007/JHEP03(2016)179 [arXiv:1512.02472 [hep-ph]].
- [30] M. Badziak, M. Olechowski and P. Szczerbiak, JHEP **1707**, 050 (2017) doi:10.1007/JHEP07(2017)050 [arXiv:1705.00227 [hep-ph]].
- [31] M. Drees and M. M. Nojiri, Phys. Rev. D **48**, 3483 (1993) doi:10.1103/PhysRevD.48.3483 [hep-ph/9307208].
- [32] M. Drees and M. M. Nojiri, Phys. Rev. D **47**, 4226 (1993) doi:10.1103/PhysRevD.47.4226 [hep-ph/9210272].
- [33] G. Belanger, F. Boudjema, A. Pukhov and A. Semenov, Comput. Phys. Commun. **180**, 747 (2009) doi:10.1016/j.cpc.2008.11.019 [arXiv:0803.2360 [hep-ph]].
- [34] Q. Riffard, F. Mayet, G. Bélanger, M.-H. Genest and D. Santos, Phys. Rev. D **93**, no. 3, 035022 (2016) doi:10.1103/PhysRevD.93.035022 [arXiv:1602.01030 [hep-ph]].

- [35] P. Huang and C. E. M. Wagner, “Blind Spots for neutralino Dark Matter in the MSSM with an intermediate m_A ,” *Phys. Rev. D* **90**, 015018(2014).
- [36] **Planck** Collaboration, N. Aghanim *et al.*, “Planck 2018 results. VI. Cosmological parameters,” *Astron. Astrophys.* **641** (2020) A6 [Erratum: *Astron. Astrophys.* 652, C4 (2021)].
- [37] J. Cao, L. Meng, Y. Yue, H. Zhou and P. Zhu, *Phys. Rev. D* **101** (2020) no.7, 075003 doi:10.1103/PhysRevD.101.075003 [arXiv:1910.14317 [hep-ph]].
- [38] T. Han, Z. Liu, and A. Natarajan, “Dark matter and Higgs bosons in the MSSM, *JHEP* **11** (2013) 008.
- [39] M. E. Cabrera, J. A. Casas, A. Delgado, *et al.*, “Naturalness of MSSM dark matter, *JHEP* **08** (2016) 058.
- [40] S. Baum, M. Carena, N. R. Shah and C. E. M. Wagner, *JHEP* **04** (2018), 069 doi:10.1007/JHEP04(2018)069 [arXiv:1712.09873 [hep-ph]].
- [41] K. Griest and D. Seckel, *Phys. Rev. D* **43**, 3191 (1991). doi:10.1103/PhysRevD.43.3191
- [42] J. R. Ellis, T. Falk, and K. A. Olive, “Neutralino - Stau coannihilation and the cosmological upper limit on the mass of the lightest supersymmetric particle, *Phys. Lett. B* **444** (1998) 367–372
- [43] J. R. Ellis, T. Falk, K. A. Olive, and M. Srednicki, “Calculations of neutralino-stau coannihilation channels and the cosmologically relevant region of MSSM parameter space,” *Astropart. Phys.* **13** (2000) 181–213, [Erratum: *Astropart. Phys.* 15, 413–414 (2001)].
- [44] M. R. Buckley, D. Hooper, and J. Kumar, “Phenomenology of Dirac Neutralino Dark Matter, *Phys. Rev. D* **88** (2013) 063532,
- [45] M. J. Baker and A. Thamm, “Leptonic WIMP Coannihilation and the Current Dark Matter Search Strategy,” *JHEP* **10** (2018) 187,
- [46] T. T. Yanagida, W. Yin, and N. Yokozaki, “Bino-wino coannihilation as a prediction in the E_7 unification of families,” *JHEP* **12** (2019) 169,
- [47] F. Feroz, M. P. Hobson and M. Bridges, *MultiNest: an efficient and robust Bayesian inference tool for cosmology and particle physics*, *Mon. Not. Roy. Astron. Soc.* **398** (2009) 1601.
- [48] K. Hagiwara, K. Ma and S. Mukhopadhyay, *Phys. Rev. D* **97** (2018) no.5, 055035.
- [49] M. Chakraborti, S. Heinemeyer and I. Saha, *Eur. Phys. J. C* **84** (2024) no.2, 165.
- [50] P. Bechtle, S. Heinemeyer, O. Stål, T. Stefaniak and G. Weiglein, *HiggsSignals: Confronting arbitrary Higgs sectors with measurements at the Tevatron and the LHC*, *Eur. Phys. J. C* **74** (2014) 2711.
- [51] O. Stål and T. Stefaniak, *Constraining extended Higgs sectors with HiggsSignals*, PoS **EPS-HEP2013** (2013) 314.
- [52] P. Bechtle, S. Heinemeyer, O. Stål, T. Stefaniak and G. Weiglein, *Probing the Standard Model with Higgs signal rates from the Tevatron, the LHC and a future ILC*, *JHEP* **11** (2014) 039.
- [53] P. Bechtle, S. Heinemeyer, T. Klingl, T. Stefaniak, G. Weiglein and J. Wittbrodt, *HiggsSignals-2: Probing new physics with precision Higgs measurements in the LHC 13 TeV era*, *Eur. Phys. J. C* **81** (2021) 145.

- [54] P. Bechtle, O. Brein, S. Heinemeyer, G. Weiglein and K. E. Williams, *HiggsBounds: Confronting Arbitrary Higgs Sectors with Exclusion Bounds from LEP and the Tevatron*, Comput. Phys. Commun. **181** (2010) 138.
- [55] P. Bechtle, O. Brein, S. Heinemeyer, G. Weiglein and K. E. Williams, *HiggsBounds 2.0.0: Confronting Neutral and Charged Higgs Sector Predictions with Exclusion Bounds from LEP and the Tevatron*, Comput. Phys. Commun. **182** (2011) 2605.
- [56] P. Bechtle, O. Brein, S. Heinemeyer, O. Stål, T. Stefaniak, G. Weiglein et al., *HiggsBounds – 4: Improved Tests of Extended Higgs Sectors against Exclusion Bounds from LEP, the Tevatron and the LHC*, Eur. Phys. J. C **74** (2014) 2693.
- [57] P. Bechtle, D. Dercks, S. Heinemeyer, T. Klingl, T. Stefaniak, G. Weiglein et al., *HiggsBounds-5: Testing Higgs Sectors in the LHC 13 TeV Era*, Eur. Phys. J. C **80** (2020) 1211.
- [58] F. Domingo, U. Ellwanger, JHEP **12**, 090 (2007) doi:10.1088/1126-6708/2007/12/090 [arXiv:0710.3714 [hep-ph]].
- [59] Domingo, and Florian, Eur. Phys. J. C **76**, no. 8, 452 (2016) doi:10.1140/epjc/s10052-016-4298-z [arXiv:1512.02091 [hep-ph]].
- [60] M. Tanabashi *et al.* [Particle Data Group], Phys. Rev. D **98** (2018) no.3, 030001 doi:10.1103/PhysRevD.98.030001
- [61] PANDAX-4T collaboration, Y. Meng et al., *Dark Matter Search Results from the PandaX-4T Commissioning Run*, Phys. Rev. Lett. **127** (2021) 261802.
- [62] XENON collaboration, E. Aprile et al., *Constraining the spin-dependent WIMP-nucleon cross sections with XENON1T*, Phys. Rev. Lett. **122** (2019) 141301.
- [63] G. Belanger, F. Boudjema, A. Pukhov and A. Semenov, *MicrOMEGAs: A Program for calculating the relic density in the MSSM*, Comput. Phys. Commun. **149** (2002) 103.
- [64] G. Belanger, F. Boudjema, C. Hugonie, A. Pukhov and A. Semenov, JCAP **0509**, 001 (2005) doi:10.1088/1475-7516/2005/09/001 [hep-ph/0505142].
- [65] G. Belanger, F. Boudjema, A. Pukhov et al. Comput. Phys. Commun. **174**, 577-604 (2006) doi:10.1016/j.cpc.2005.12.005 [arXiv:04052537 [hep-ph]].
- [66] G. Belanger, F. Boudjema, A. Pukhov et al. Comput. Phys. Commun. **176**, 367-382 (2007) doi:10.1016/j.cpc.2006.11.008 [arXiv:0607059 [hep-ph]].
- [67] G. Belanger, F. Boudjema, A. Pukhov and A. Semenov, *micrOMEGAs: A Tool for dark matter studies*, Nuovo Cim. C **033N2** (2010) 111.
- [68] G. Belanger, F. Boudjema, A. Pukhov et al. Comput. Phys. Commun. **185**, 960-985 (2014) doi:10.1016/j.cpc.2013.10.016 [arXiv:1305.0237 [hep-ph]].
- [69] D. Barducci, G. Belanger, J. Bernon, F. Boudjema, J. Da Silva, S. Kraml et al., *Collider limits on new physics within micrOMEGAs*, [arXiv:1606.03834 [hep-ph]].
- [70] G. Belanger, F. Boudjema, A. Goudelis et al. Comput. Phys. Commun. **231**, 173-186 (2018) doi:10.1016/j.cpc.2018.04.027 [arXiv:1801.03509 [hep-ph]].
- [71] J. E. Camargo-Molina, B. O’Leary, W. Porod and F. Staub, *Vevacious: A Tool For Finding The Global Minima Of One-Loop Effective Potentials With Many Scalars*, Eur. Phys. J. C **73** (2013) 2588.

- [72] J. E. Camargo-Molina, B. Garbrecht, B. O’Leary, W. Porod and F. Staub, *Constraining the Natural MSSM through tunneling to color-breaking vacua at zero and non-zero temperature*, Phys. Lett. B **737** (2014) 156.
- [73] MUON G-2 collaboration, G. W. Bennett et al., *Phys. Rev. D* **73** (2006) 072003.
- [74] B. Abi *et al.* [Muon g-2], Phys. Rev. Lett. **126** (2021) no.14, 141801
doi:10.1103/PhysRevLett.126.141801 [arXiv:2104.03281 [hep-ex]].
- [75] T. Aoyama, N. Asmussen, M. Benayoun, J. Bijnens, T. Blum, M. Bruno, I. Caprini, C. M. Carloni Calame, M. Cè and G. Colangelo, *et al.* Phys. Rept. **887** (2020), 1-166
doi:10.1016/j.physrep.2020.07.006 [arXiv:2006.04822 [hep-ph]].